PERGAMON

International Journal of Heat and Mass Transfer 45 (2002) 1983–1991

International Journal of HEAT and MASS TRANSFER

www.elsevier.com/locate/ijhmt

Determination of the temperature and concentrations for the products of combustion of a hydrocarbon fuel on the basis of their infrared self-radiation

E. Vitkin [a], O. Zhdanovich [a], V. Tamanovich [a,*], V. Senchenko [b], V. Dozhdikov [b], M. Ignatiev [c], I. Smurov [d]

[a] *Institute of Physics, National Academy of Sciences of Belarus, 68 F. Skarina Av., 220072 Minsk, Belarus*
[b] *Institute of Thermodynamics of Extreme Conditions, Russian Academy of Sciences, 13/19 Izhorskaya Str., 127412 Moscow, Russia*
[c] *A.A. Baikov Institute of Metallurgy, Russian Academy of Sciences, 49 Leninskiy Av., 117911 Moscow, Russia*
[d] *Ecole Nationale d'Ingénieurs de Saint-Etienne, 58 rue Jean Parot, 42023 Saint-Etienne Cedex, France*

Received 27 December 2000

Abstract

A measuring system has been developed and a procedure has been proposed for determining the temperature of gas flows and the concentrations of the products of combustion of organic fuels on the basis of the spectral "radiation–absorption" method. A gas multi-wavelength (1.8–4.8 μm) pyrometer–photometer has been created for measuring the self-radiation of gas flows and transmission of probing radiation from a reference source. The optimization of spectral intervals for temperature measurements of combustion products has been made. The test results of the temperature measurements for a laboratory gas burner are presented.

1. Introduction

The users of combustion technologies demand reduction in the impact of the invasion of pollutants along with a decrease of fuel losses. The main technological problem is to reach maximum completeness of combustion and to avoid flame temperature instabilities that affect both fuel consumption and radiation of toxic components (CO_x, NO_x, etc.). A reliable spatially resolved on-line temperature measurement technique allows a better general understanding of combustion processes and their optimization. In recent years, optical methods [1], in which self-radiation of combustion products is used, and methods of laser diagnostics have come to widespread use. The former are the radiation–absorption methods or the Schmidt method, the method of spectral line reversal, and various combinations of these methods. The laser methods include both laser-Doppler velocimetry (LDV) and variations of image velocimetry (IV) for characterization of flow and Rayleigh scattering, spontaneous Raman spectroscopy (SRS), coherent anti-Stokes Raman spectroscopy (CARS), and laser-induced fluorescence (LIF) for quantification of temperature and concentration. These methods are both accurate and sensitive for fundamental research of concentrations of combustion products and of flame temperature. However, there are some serious limitations hampering their wide industrial applications: lack of protection against the influence of harsh environment, greatest difficulties posed by assembling under industrial conditions, and a very high cost.

In diagnosing flows of a heated molecular gas, such as flames, gas sprays of combustion products, and so on, the characteristics of their thermal radiation, which possess high informativeness, can be used with great effectiveness. However, the relationship between optical characteristics of radiating volume and thermodynamic parameters of a flow is very complex due to the non-uniformity of gas-dynamic fields, high selectivity of radiation, and its reabsorption. In traditional approaches to diagnostics of flames on the basis of their

* Corresponding author. Tel.: +7-375-172-8424-49.
E-mail address: evitkin@dragon.bas-net.by (V. Tamanovich).

0017-9310/02/$ - see front matter
PII: S0017-9310(01)00139-9

Nomenclature

Br	spectral density of energetic brightness
C	concentration of radiating gas
E	energy of the lower state
g_0	relative half-width of a spread function
R	transmittance of a layer
T	temperature
$T_n(\lambda)$	spread function of a device
X	thickness of radiating layer

Greek symbols

α	stoichiometry of a fuel–air mixture
λ	wavelength
σ	correlation length for an absolute error

self-radiation, temperature non-uniformity of the medium along the measurement beam is usually not taken into account. Therefore such a physical model of radiation–absorption method has been developed in the present work which enables one to take into account heated and cold radiating layers in optical diagnostics of flames and in which the amount of computations is brought to the level acceptable for industrial conditions. For the implementation of the method, a relatively inexpensive diagnostic equipment has been created, which is adaptable to industrial equipment, namely, an infrared gas multi-wavelength pyrometer that includes a special water-cooled optical fibre probe, which can be easily introduced in any zone of an industrial furnace. Software has also been developed, which enables one to determine temperatures and concentrations of combustion products from measured spectral brightnesses in a wide range of wavelengths.

2. Calculation of radiation transfer in rovibrational bands of molecules

The spectral density of energetic brightness (SDEB) of flames in thermal-power engineering apparatuses is to be calculated in the problems of optical diagnostics with regard for radiation transfer along a large number of beams. In connection with this, the time of calculation of one beam is of principal importance. The methods based on consideration of the real structure of rovibrational bands and on models that take into account the overlapping of lines and, all the more, the methods of spectral integration along a contour of lines [2] become very cumbersome for such problems. Moreover, they cannot be easily adapted to molecules whose rovibrational spectra have a complex structure.

At the present time, the method proposed by Curtis and Godson (the CG method) has gained the most wide acceptance for radiation transfer calculations on a mass scale. This method that proved its effectiveness in the problems of atmospheric optics in application to isothermal atmospheric paths was later extended to non-isothermal volumes of molecular gases [3]. The essence of the method is that transmittance along a non-uniform path is replaced by transmittance of a certain equivalent uniform layer. In the limiting cases of weak and strong lines, the transmittances of the real and uniform layers coincide exactly. But in the range of parameters where these approximations do not hold, this kind of replacement leads to errors. However, numerous calculations based on the CG method and carried out exactly, and also comparisons with experiment show that in most cases of weakly non-isothermal paths the CG method approximation ensures a satisfactory accuracy in an intermediate range too.

In the case of the statistical model, the transmittance of an uniform layer is expressed in terms of two parameters: the mean absorption coefficient, S/d, and the parameter of the density of lines, γ/d. The standard procedure of extending the results which are valid for uniform layers to the case of non-uniform path consists in the use of the values $\overline{S/d}$ and $\overline{\gamma/d}$ averaged along the optical path. The temperature dependences of S/d and γ/d are determined by all the lines entering into the given spectral interval. The introduction of such a two-parameter description is equivalent to the replacement of a combination of real lines by a set of identical lines with a certain model dependence of equivalent width on line strength and optical thickness, and also of the line strength on temperature. It is obvious that this replacement in calculations results in the disregard of the radiation of "hot lines" along non-uniform paths, i.e. the lines which correspond to transitions between states with high energy values and are weakly adsorbed in the low-temperature parts of the path.

This drawback can be obviated by introducing averaged parameters not for all the lines in the given spectral interval, but separately for each group of lines with close values of energy of the lower states [4]. The procedure corresponds to the introduction of J groups of lines with a definite weight for each group, which is equal to the number of lines in the given group. This approach is intermediate between a one-group description with the use of S/d and γ/d and an exact description of each line. Within the limits of this approach, the spectral density of energetic brightness Br and the transmittance R of the layer of thickness L are written in the form

$$Br(L) = Br^0 R(L) + \int_0^L B^0(x)\,\mathrm{d}R(x), \tag{1a}$$

$$R(x) = \exp\left(-\sum_{j=1}^{J} W_j \Big/ \sqrt{1 + W_j^2/4V_j} \right), \tag{1b}$$

$$W_j = \int_0^X N_j M_j \exp(-E_j/T(x)) C(x)\,\mathrm{d}x, \tag{1c}$$

$$V_j = N_j \int_0^X \gamma(x) N_j M_j \exp(-E_j/T(x)) C(x)\,\mathrm{d}x. \tag{1d}$$

Here $T(x)$ and $C(x)$ are the temperature and concentration of a component at the point x of the layer; B^0 is the brightness of the equilibrium radiation (the Planck function); Br^0 is the background brightness; J is the number of groups; N_j, M_j, and E_j are the parameters of groups with the following physical sense; N_j is the number of lines, M_j is the matrix element, E_j is the energy of the lower state. If it would be possible to describe the position of each line exactly, the parameters could have been calculated for an arbitrary number of groups and arbitrary division with respect to energies depending on the required accuracy. However, the initial data (the position and strength of the lines, contour shape) are known with some error, especially for high temperatures, and there is no sense in taking into account approximate data exactly.

There are a number of different methods for determining group parameters that differ in both the character of the input information used and mathematical procedure. The parameters of the groups were determined in [4] on the basis of experimental data for transmittance of uniform layers at temperatures above 1000 K and from direct calculations in terms of the parameters of lines for lower temperatures. An algorithm was used for obtaining parameters of a multi-level model adapted specially for the problems of filter diagnostics from radiometric measurements of thermal self-radiation. A requirement concerning an adequate description of a certain functional dependence of the spectral characteristics of flows on their thermodynamic parameters Y_j is identical to obtaining the global minimum of the following functional:

$$F(Y_j) = \sum_i g_i \left[\frac{1 - A_i}{R_i(Y_j)} - 1 \right]^2, \tag{2}$$

where R_i is the spectral transmittance of the ith layer calculated from Eqs. (1a)–(1d); A_i is the value of spectral absorption obtained for the same object experimentally or calculated theoretically according to the exact model; g_i is the characteristic of the authenticity of the value A_i. The objects i must overlap the entire range of the possible parameters. In practice, the maximum possible number of objects and, consequently, of equations is limited by admissible expenditures of machine time. The calculations carried out showed that the spectral characteristics of molecular gases could be described by means of nine parameters in the temperature range 250–2500 K for the spectral interval $\lambda = 2$–25 μm and the range of absorbing masses which is typical of the problems concerned with calculation of radiation transfer of heated gas layers through a cold air layer with an error not exceeding 12%.

In simulation of experimental investigations of the spectral characteristics of objects, it is necessary to carry out averaging over the spread function of a specific measuring device:

$$R_n = \frac{\int_{-\infty}^{\infty} R(\lambda) T_n(\lambda)\,\mathrm{d}\lambda}{\int_{-\infty}^{\infty} T_n(\lambda)\,\mathrm{d}\lambda}, \tag{3}$$

where $T_n(\lambda)$ is the spread function of the device for the measuring channel n. The necessity of taking into account the spread function complicates the numerical procedure of radiation transfer calculation. To simplify the problem, we will proceed in the following way: we will write the transmittance within the limits of the filter using certain mean-square (over the filter) parameters of the multi-level model. These parameters will be found from the condition of coincidence of the transmittance in the form of Eq. (1b) with that expressed via mean parameters in the limiting approximations of an absolutely thin and thick lines.

3. Method of diagnostics of temperature and concentrations on the basis of self-radiation

We assume that the object investigated is an uniform gas layer of thickness X_h and temperature T, with the water vapour and carbon dioxide being radiating components whose mole concentrations are $C_{\mathrm{H_2O}}$ and $C_{\mathrm{CO_2}}$. The spectral density of energetic brightness $\mathrm{Br}(\lambda_n)$ is measured through a cold air layer of thickness X_c in the range $\lambda = 1.8$–4.8 μm by a filter spectrometer in M channels with different wavelengths and a given spread function $T_n(\lambda)$.

A special procedure based on finding the minimum of the discrepancy between the experimentally measured radiation brightness Be_n and that calculated Bt_n has been developed for recovering the temperature and concentrations in the radiating layer from the measured SDEB. The functional dependences of Bt_n on temperature T and the concentrations of radiating components $C_{\mathrm{H_2O}}$ and $C_{\mathrm{CO_2}}$ are determined for each channel in accordance with the three-level model described by relations (1a)–(1d). The minimization problem of the following form is being solved:

$$\sum_n (\beta_n(\mathrm{Be}_n - \mathrm{Bt}_n))^2 \;\Rightarrow\; \min, \tag{4}$$

where $\sum$ indicates summation over all the channels of measurement and β_n are the weight multipliers.

In numerical realization of the procedure, technical difficulties arose due to the complexity and nonlinearity of the model of calculation of SDEB, in particular, to the presence of a number of local minima in expression (4). We did not succeed in finding a suitable standard program of optimization. Therefore, a special algorithm has been developed which is based on the adjustment to temperature and on SVD factorization for Eqs. (1a)–(1d) linearized with respect to concentrations.

Mathematical simulation was used to investigate the influence of inevitable errors in measurement of SDEB on the recovered values of temperature and concentrations of radiating components. We will limit ourselves to the analysis of the simplest spread functions that have the Lorentzian

$$T_n(\lambda) = g \Big/ \left\{ \pi \left(1 + \left(\frac{\lambda - \lambda_n}{g} \right)^2 \right) \right\} \tag{5}$$

or Doppler

$$T_n(\lambda) = \frac{g}{\sqrt{\pi}} \exp\left(- \left(\frac{\lambda - \lambda_n}{g} \right)^2 \right) \tag{6}$$

contours with the relative half-width $g_0 = g/\lambda_n$. Suppose measurement in each channel is carried out with the random error

$$b_n = \mathrm{Rr}_n \mathrm{Br}(\lambda_n) + \mathrm{Ra}_n B_{\max}, \tag{7}$$

where Rr_n are the pseudorandom numbers distributed uniformly in the range $(-\mathrm{Rr})$–$(+\mathrm{Rr})$; Ra_n is the sequence of the numbers distributed in the range $(-\mathrm{Ra})$–$(+\mathrm{Ra})$ with the correlation length σ between the channels. Then the "experimental" spectrum is given by the values

$$\mathrm{Be}_n = \mathrm{Br}(\lambda_n) + b_n. \tag{8}$$

Thus distorted brightness values of flow radiation are used for solving problem (4). Random selection of variants of initial conditions is carried out by means of the generator of random numbers distributed according to the normal law with a mean-square error determined by expression (7). The solution yields values of the temperature T_t and concentrations $C_{\mathrm{H_2Ot}}$ and $C_{\mathrm{CO_2t}}$ that correspond to the concrete realization of the experimental spectrum (8).

Fig. 1 illustrates the procedure described. For each of the temperatures of 1000, 1500, and 2000 K the values of brightness are given for one of the experimental realizations (markers) and also theoretical spectra constructed for the parameters determined by the diagnostic procedure.

The errors in determining the parameters for this realization are given by the values $\delta T = T_\mathrm{t} - T$, $\delta H = C_{\mathrm{H_2Ot}} - C_{\mathrm{H_2O}}$, and $\delta C = C_{\mathrm{CO_2t}} - C_{\mathrm{CO_2}}$. And, finally, the values averaged over an ensemble of J realizations

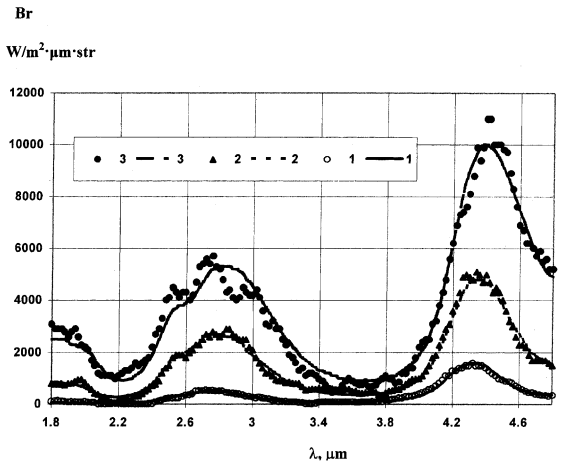

Fig. 1. Experimental (markers) and calculated (lines) spectra of radiation brightness for the temperatures: (1) 1000 K, (2) 1500 K and (3) 2000 K .

$$\delta T = \sqrt{\frac{\sum_j \delta T_j^2}{J}}, \quad \delta H = \sqrt{\frac{\sum_j \delta H_j^2}{J}}, \quad \delta C = \sqrt{\frac{\sum_j \delta C_j^2}{J}} \tag{9}$$

that are found by means of J-multiple repetition of the procedure described can be considered as estimates of mean-square errors in determining temperature and concentrations in accordance with this procedure.

A good coincidence between the recovered concentrations of radiating components and temperature and the calculated values for a wide range of parameters without any special adaptation of the calculation procedure for radiation transfer to the experimental scheme indicates the correctness of the selected algorithm for recovery. There are grounds to expect that after an additional analysis concerning the selection of spectral points, resolution, and accuracy of the characteristics of measuring apparatus, the method suggested will enable one to determine the characteristics of combustion products of thermal-power engineering apparatuses with a fairly high accuracy.

4. Dependence of the errors for recovery on the accuracy of brightness measurement

When measurement errors are not too large, for the function that specifies the dependence of SDEB on the temperature and concentrations of radiating components it is possible to use, in an explicit form, linearization near the mean value and obtain a simple dependence of the errors of recovery on the

measurement accuracy. It is easier to present the method in a general form.

Suppose that M parameters of the theoretical model $\mathbf{P}_0$, $\{p_{0,1},\ldots p_{0,m},\ldots,p_{0,M}\}$, correspond to the exact value of brightness. We will use Taylor expansion for each channel $n=1,\ldots,N$ in the zone investigated:

$$\mathrm{Bt}_n(\mathbf{P}) = \mathrm{Bt}_n(\mathbf{P}_0) + \sum_{m=1}^{M} \frac{\partial \mathrm{Bt}_n(\mathbf{P}_0)}{\partial p_m}\Delta_m,$$
$$\Delta_m = p_m - p_{0,m} \tag{10}$$

and the measurement error is simulated according to formulae (7) and (8). Using the idea of the least-square method, we will obtain the following functional instead of expression (4):

$$\sum_{n=1}^{N}\left[\mathrm{Rr}_n\mathrm{Br}(\lambda_n)+\mathrm{Ra}_n B_{\max}-\sum_{m=1}^{M}\frac{\partial \mathrm{Bt}_n(\mathbf{P}_0)}{\partial p_m}\Delta_m\right]^2\beta_n \Rightarrow \min. \tag{11}$$

Differentiating relation (11) with respect to the increments Δ_m, we arrive at the system of M linear equations for Δ_k:

$$\sum_{k=1}^{M} c_{ik}\Delta_k = B1_i + B2_i, \quad i=1,2,3,\ldots,M, \tag{12}$$

where

$$c_{ik} = \sum_{n=1}^{N}\beta_n \frac{\partial \mathrm{Bt}_n(\mathbf{P}_0)}{\partial p_i}\frac{\partial \mathrm{Bt}_n(\mathbf{P}_0)}{\partial p_k},$$
$$B1_i = \mathrm{Rr}\sum_{n=1}^{N}\beta_n\omega_n\mathrm{Br}(\lambda_n)\frac{\partial \mathrm{Bt}_n(\mathbf{P}_0)}{\partial p_i},$$
$$B2_i = \mathrm{Ra}B_{\max}\sum_{n=1}^{N}\beta_n\psi_n\frac{\partial \mathrm{Bt}_n(\mathbf{P}_0)}{\partial p_i}.$$

In the above expressions for the right-hand sides $B1$ and $B2$, the amplitudes of random sequences, Rr and Ra, are specially isolated, so that now ω_n are the random numbers uniformly distributed in the interval (-1)–$(+1)$, ψ_n is the sequence of the numbers that mutually correlate with a given correlation length σ.

The solution of the system of equations (12) is

$$\Delta_k = c_{ik}^{-1}\cdot(B1_i + B2_i), \tag{13}$$

that is, the value of the error in the determination of the system parameter p_k in one of the realizations of numerical experiment dealing with the SDEB measurement. To estimate a probable error, it is necessary to carry out the averaging of Eq. (13) over a large number of realizations, which leads to the dependence

$$\delta_k = \sqrt{(\mathrm{Rr}C1_k)^2 + (\mathrm{Ra}C2_k)^2}, \tag{14}$$

in which the coefficients $C1_k$ and $C2_k$ depend only on mean values of the parameters of the measured system $\mathbf{P}_0$ and correlation length for the absolute error σ and can be called as the rate of increase of error in determination of the parameter p_k depending on the values of the relative and absolute measurement errors, respectively.

For our problem, the parameters are the temperatures and concentrations of H_2O and CO_2. For a specific experimental situation, the procedure stated allows one to calculate the coefficients $C1_\mathrm{T}$, $C1_\mathrm{H}$, $C1_\mathrm{C}$ and $C2_\mathrm{T}$, $C2_\mathrm{H}$, $C2_\mathrm{C}$ that specify the dependences of possible mean-square relative errors in diagnostics of temperature δ_T, concentrations of water δ_H and of carbon dioxide δ_C from the measured SDEB depending on the relative (Rr) and absolute (Ra) errors:

$$\delta_\mathrm{T} = \sqrt{(\mathrm{Rr}C1_\mathrm{T})^2 + (\mathrm{Ra}C2_\mathrm{T})^2},$$
$$\delta_\mathrm{H} = \sqrt{(\mathrm{Rr}C1_\mathrm{H})^2 + (\mathrm{Ra}C2_\mathrm{H})^2}, \tag{15}$$
$$\delta_\mathrm{C} = \sqrt{(\mathrm{Rr}C1_\mathrm{C})^2 + (\mathrm{Ra}C2_\mathrm{C})^2}.$$

These dependences are very useful in the stage of design and adjustment of special diagnostic apparatus. Below, the figures give the results of calculations of $C1_k$ and $C2_k$ for the characteristics of a special filter spectrometer and conditions of measurement described in what follows.

The calculations were carried out for the following parameters: the spread function contour is the Lorentzian and Doppler; relative half-width of the contour $g_0 = 0.02$; thickness of the hot layer $X_\mathrm{h} = 0.18$ m; that of the cold layer $X_\mathrm{c} = 0.1$ m; $T = 1500$ K. Here, in calculation of the rate of error change depending on relative errors of measurement, $C1_k$, correlation was not used, and the rates of change in errors depending on absolute errors, $C2_k$, were calculated with the correlation $\sigma = 0, 0.1$, and 0.5.

The behaviour of the dependences of $C1_k$ and $C2_k$ on the spread function half-width upon change of the latter from 0.01 to 0.2 is approximately the same for the errors in determining temperature and concentrations. A smooth increase in the values of $C2_k$ is observed with increase in the half-width, except for the range of half-widths 0.05–0.1 where there is an unexplainable fluctuation of $C2_\mathrm{T}$ in 0.1 and 0.5 correlations. The $C1_k$ values depend weakly on the half-width of the spread function for the Lorentzian contour and virtually do not depend on that with the Doppler contour. The values of $C1_k$ and $C2_k$ are always higher for the spread function with the Lorentzian contour. The discrepancy increases with increasing half-width. Fig. 2 shows the dependences of $C1_\mathrm{T}$ and $C2_\mathrm{T}$ on the relative half-width of the spread function for the Lorentzian and Doppler forms of the contour.

The values of $C1_\mathrm{T}$ and $C2_\mathrm{T}$ increase with temperature up to the value 1300 K. With a further rise in temperature, the increase of $C1_\mathrm{T}$ and $C2_\mathrm{T}$ becomes slower, and

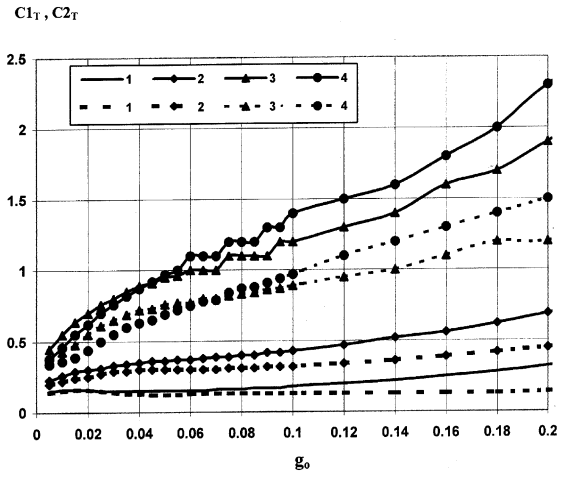

Fig. 2. Dependences of the parameters $C1_T$ (1) and $C2_T$ for the correlation values $\sigma = 0$ (2), 0.1 (3), and 0.5 (4) on the spread function half-width for the Lorentzian (solid lines) and Doppler (dashed lines) contours of the spread function.

the values of $C2_T$ calculated with zero correlation do not depend practically on temperature. The values of $C2_H$ decrease sharply with increase in temperature from 500 to 900 K and very slowly with a further increase in temperature. The values of $C1_H$ do not depend practically on T. The dependence on the shape of the contour is seen only at temperatures lower than 1000 K. The higher the temperature, the smaller the values of $C1_C$ and $C2_C$. Fig. 3 shows the dependences of $C1_T$ and $C2_T$ on temperature for the spread function with the Lorentzian and Doppler contours.

All the dependences of $C1_k$ and $C2_k$ on the thickness of the hot layer X_h have a distinct maximum at

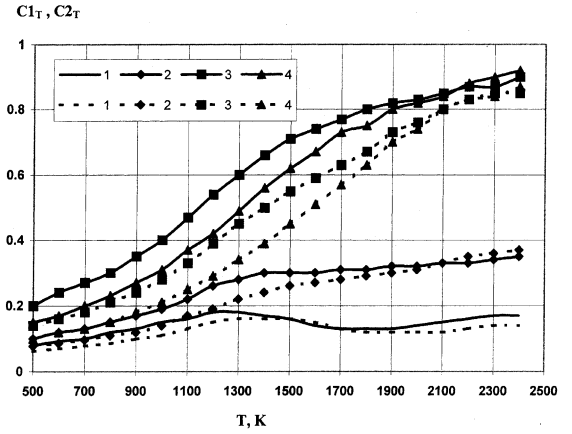

Fig. 3. Dependences of the parameters $C1_T$ (1) and $C2_T$ for the correlation values $\sigma = 0$ (2), 0.1 (3), and 0.5 (4) on temperature for the Lorentzian (solid lines) and Doppler (dashed lines) contours of the spread function.

$X_h \approx 0.1$ m. After passing the minimum at $X_h \approx 0.7$ m, the values of the coefficients increase smoothly with X_h. They increase with the thickness of the cold layer up to $X_c \approx 200$ m and do not practically change with further increase in X_c.

All the above-mentioned regularities and estimates are related to the "internal" errors of the model. Practical implementation of the procedure is inevitably connected with departure from the model, which can lead to additional errors in determining temperatures and concentrations. The errors in the diagnostics may mainly arise from: radiation sources that are not taken into account in calculations, such as absorbing components in combustion products, background illuminations, and scattering by particles; departures from calculated geometry, namely, non-uniformities in a radiating layer and inexact specification of the parameters of an absorbing layer; inaccuracies in setting the spread function in the channels of a receiver and errors in their graduation, etc.

5. Construction of the device

The measuring system consists of a multi-wavelength pyrometer, a unit of infrared radiation reference source for preliminary illumination, and an external optical probe. The block diagram of the measuring system on the basis of the gas multi-wavelength pyrometer is presented in Fig. 4. The gas pyrometer is a scanning infrared spectrometer connected with the optical probe by means of an infrared optical fibre. The device is placed into a closed metal box, which can be blown-through with an inert gas. The monochromator of the gas pyrometer has a relative spectral resolution of 2–2.5% and operates in the spectral range 1.8–4.8 μm. The entrance slit is formed by the face of the infrared optical fibre that connects the spectrometer with the external probe. A variable-density interference filter located behind the entrance slit of the device is used as a dispersive element. Radiation from the entrance slit that passed through the variable-density interference filter is collected on the active area of the IR photodetector by means of a CaF_2 lens. A PbSe photodiode on heterostructure is used as a photodetector. An active element of the photodiode is placed on the cold junction of an integral two-stage Peltier cooler. The temperature of the cold junction is kept up equal to $-(45 \pm 0.1)^{\circ}$C and controlled by a thermoresistor fixed near the active element. The range of spectral sensitivity of the photodetector at the level 0.2 is 1.0–4.9 μ. The photodiode has the detectivity $D^* \cong 10^{10}$ W^{-1} cm Hz$^{1/2}$ at the maximum of spectral sensitivity. Photocurrent produced by the photodiode D1 is amplified by a low-noise transimpedance preamplifier and is directed to the amplifier unit with automatic zero adjustment of a dark signal of the diode.

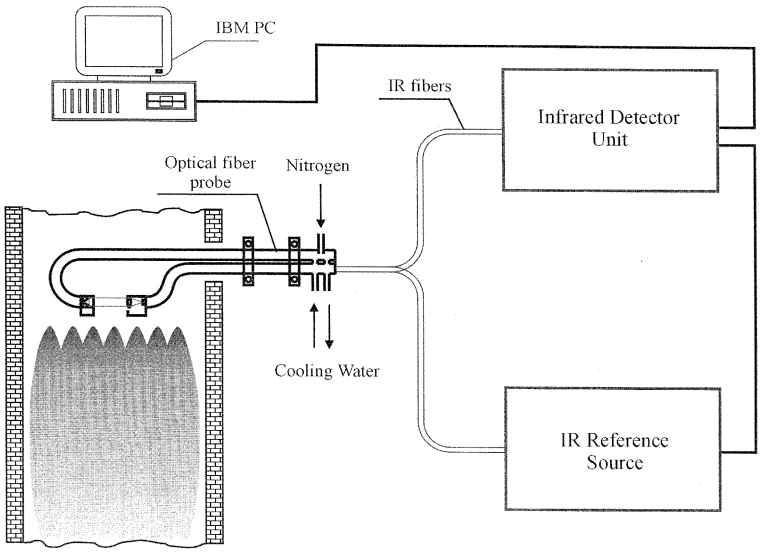

Fig. 4. Block diagram of the measuring system for the control of temperature on the furnace of closed type.

Thereafter, the signal through a scaling amplifier enters a two-channel 12-bit analog–digital converter. The data acquisition system of the pyrometer is based on a digital signal processor which calculates brightness temperatures, stores the results of measurements in internal random memory, and sends them to an IBM-type personal computer via an RS232 interface.

Scanning over spectrum is made by a rotating variable-density filter with a rotation frequency of 50 Hz. The spectral characteristics of transmittance of the filter versus the wavelength (angle of rotation) are presented in Fig. 5.

A tungsten halogen lamp with a sapphire window and mirror collecting optics is used as an infrared source. Stability of radiation energy is ensured at a level of 10^{-4} by stabilizing the heating current through the lamp filament. The infrared source unit is a closed casing that can be blown-through with an inert gas, where the lamp, the power unit, and control electronics are placed. Radiation from the halogen lamp is focused on the face of the infrared optical fibre connected with the external optical probe. Radiant flux is modulated with a frequency of 12–16 Hz by means of a chopper.

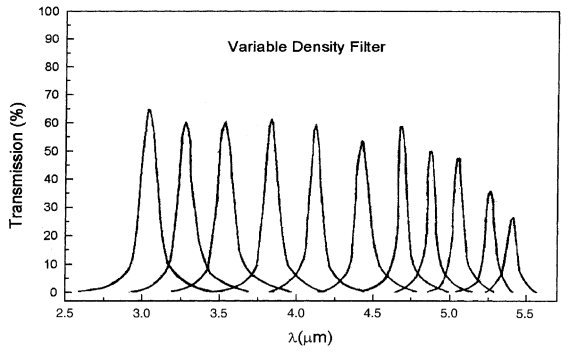

Fig. 5. Dependence of the spectral transmittance of the interference filter on wavelength.

The optical fibre probe is a steel rod cooled by water and blown-through with nitrogen; in its interior an optical system for measurements of self-radiation and absorption of combustion products is placed. The optical probe can be easily introduced into any zone of an industrial furnace by means of a robot-manipulator.

The spread function of the device used in calculations was measured on a special experimental stand consisting of a double prismatic monochromator, a stable black body model-type IR source with a working temperature of (2500 ± 0.5) K, and the non-selective IR detector of radiation that controls radiation power. The spread function obtained in this way was approximated by two modified Lorentzian functions at 208 wavelengths within the range 1.8–4.8 μm separately for the left- and the right-branches. This approach enables one to determine special parameters of groups for calculation of radiation transfer (in accordance with the procedure presented in [3]).

The pyrometer was calibrated both in intensity units and in brightness temperature according to the black body model in the temperature range 700–1800 K.

6. Experimental investigations on a flat burner

To verify the computational procedure, experiments were carried out with measurement of SDEB and transmittance on an experimental burner. The burner

was of closed type and had practically a flat temperature profile along the line of sight. The measurements were carried out along the line of sight along the burner axis at the points with different Y and Z coordinates. Size of the burner along line of sight was equal to 180 mm. The output power P of the burner was in range 3.0–3.5 kW.

The burner was supplied with a special system of preliminary mixing of a fuel and an oxidant; the system also contributed to the stabilization of flow of this mixture. Thus, the burner gave a low-turbulent and stable flame. The temperature was measured with different stoichiometry of the fuel–air mixture, α, where

$$\alpha = Q_{\text{air}}/Q_{\text{air in stoichiometric combustion}}.$$

Here α_{air} is the primary air flow, and the value in the denominator gives the air flow corresponding to complete (stoichiometric) combustion.

To decrease the content of NO_x and CO in combustion products, the secondary (additional) flow Q_s of cold air was supplied to the burner, and this flow was characterized by the coefficient α_s:

$$\alpha_s = Q_s/Q_{\text{air}}\ (\%).$$

The temperature of the burner was measured with use of optical fibre probe depicted in Fig. 4. This probe has a fixed distance between the objectives of 280 mm and a rigid structure. During measurements, the fasteners of the objectives were not influenced by the burner flame. The diameter of a probing beam was 6 mm.

The results of measurements were processed by the above-described procedure, with transmittance taken into account, and by a modified spectral radiation–absorption method [5].

The radiation–absorption method was used for direct calculation of temperature from measured brightness temperature and attenuation in the 2.7 μm band where the influence of atmospheric water and CO_2 was at minimum. To determine the temperature, a range of wavelength is selected on the long-wavelength wing of the spectral band of 2.7 μm where absorption occurs in the "hot" lines of CO_2 and water. The device recorded the spectral intensities (Fig. 6(a)), from which effective brightness temperatures were calculated and then the gas temperatures over the region of the local maximum of absorption was determined (Fig. 6(b)). For the temperature 1000–2300 K the absorption maximum lay within the limits 2.8–2.9 μm. The pyrometer showed a

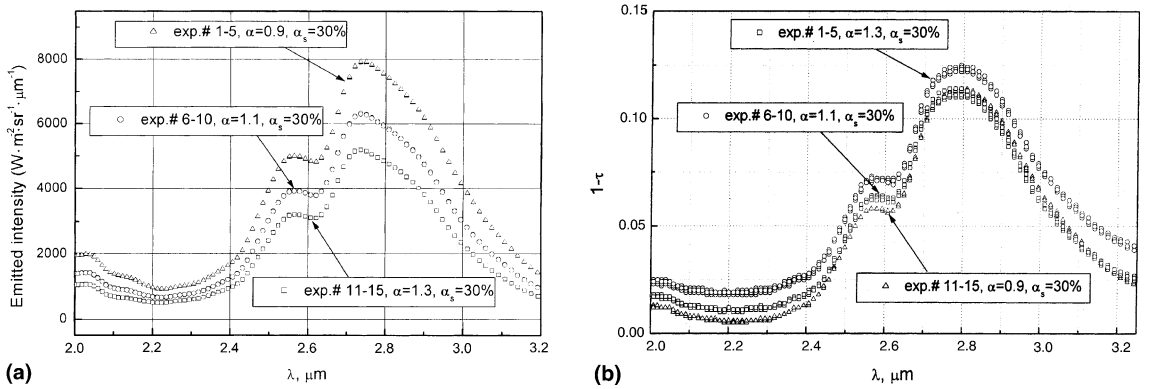

Fig. 6. (a) The temperature of combustion products in the vicinity of the 2.7 μm band determined by the radiation–absorption method. (b) Spectral dependence of the absorption of combustion products in the vicinity of the 2.7 μm band.

Table 1
The values of temperature recovered from measurements (T^{I} and T^{II}) and determined by the radiation–absorption method (T^{III})

Number of experiment	Z (mm)	Y (mm)	P (kW)	α	α_s (%)	T^{I} (K)	T^{II} (K)	T^{III} (K)	Noise (rms, K)
1–5	9	0	3.42	0.9	30	1987	2142	2110	5
6–10	9	0	3.42	1.1	30	1850	1886	1872	5
11–15	9	0	3.42	1.3	30	1747	1826	1813	7
16–20	9	0	3.00	1.3	0	1785	1852	1837	4
21–25	9	0	3.00	1.1	0	1963	2031	2017	7
41–45	9	0	3.42	1.1	30	1850	1886	1872	5
46–50	9	0	3.42	1.3	30	1747	1826	1813	7
51–55	9	0	3.00	1.3	0	1785	1852	1837	4

high stability of measurements and their excellent reproducibility for all the regimes of the burner operation. All the measurements were fulfilled with averaging 10 spectra during 0.6 s.

Table 1 presents the temperatures recovered from the measured SDEB and transmittance (T^{I}), only from SDEB (T^{II}), and those calculated by the spectral radiation–absorption method (T^{III}). The value of the standard departure for the temperature T^{III} determined by the radiation–absorption method is given in the column "Noise". The "P" column lists the output power of the burner under different operating conditions.

7. Conclusions

Noticeable differences in determining temperature by methods I and II are explained, apparently, by a systematic error arising in simulation of transmission. To eliminate simulation errors, the measuring system must be adapted to the measurement conditions by means of control measurements and determination of calculated constants (weight coefficients β_n in Eq. (4)) from these measurements. A good coincidence of the temperature calculated from brightness and that determined by the method of spectral radiation–absorption should be noted. Thus, the difference between these temperatures is approximately equal to 15° and is of systematic character.

The comparison carried out demonstrates the usefulness of the proposed method for recovering the temperature and concentrations of radiating components in real technological equipment. It is to be expected that the accuracy and reliability of the results suggested can be substantially increased by purposefully selecting spectral ranges and parameters of recording devices by the method of mathematical simulation. Of great interest is the development of a reliable procedure and a simple wide-band filter device operating in the 2.7 μm band with the use of optical fibre probes that decrease the influence of atmospheric CO_2 and water.

References

[1] E.P. Hassel, S. Linow, Laser diagnostics for studies of turbulent combustion, Measure. Sci. Technol. 11 (2000) R37–R57.

[2] R.M. Goody, Atmospheric Radiation, Oxford University Press, Oxford, 1964.

[3] C.B. Ludwig, W. Malkmus, J.E. Reardon, J.A.L. Thompson, Handbook of infrared radiation from combustion gases, NASA report Sp-3080, 1980, p. 386.

[4] E.I. Vitkin, S.L. Shuralyov, V.V. Tamanovich, Engineering procedure for calculating the transfer of the selective radiation of molecular gases, Int. J. Heat Mass Transfer 43 (2000) 2029–2045.

[5] V.I. Vladimirov, Yu.A. Gorshkov, V.S. Dozhdikov, V.N. Senchenko, A brightness pyrometer technique for temperature measurements in the flames of hydrocarbon fuels, in: Proceedings of the First International Symposium on Radiation Transfer, Kusadasi, Turkey, August 13–18, 1995, pp. 627–634.